J. Membrane Biol. 205, 81–88 (2005)
DOI: 10.1007/s00232-005-0765-4

The Journal of
Membrane
Biology

Non-Stationary Fluctuation Analysis of Macroscopic Gap Junction Channel Records

S.V. Ramanan[1], **V. Valiunas**[2], **P.R. Brink**[2]
[1]AU-KBC Research Center, MIT, Chromepet, Chennai 600044, India
[2]Physiology and Biophysics, SUNY at Stony Brook, NY 11794-8661, USA

Received: 25 March 2005/Revised: 4 August 2005

Abstract. Non-stationary fluctuation analysis was applied to macroscopic records of junctional currents arising from homotypic Cx37 and Cx43 gap junction channels expressed in RIN cells. The data were analyzed by a modification of existing analytical methods that takes endemic uncoupling into account. The results are consistent with both channels having open probabilities ranging from 0.7 to near unity for low transjunctional voltages. The analysis also yielded estimates of single-channel conductances for the two channel types similar to those seen in single-channel recordings. The results presented here show that fluctuation analysis can be used to extract single-channel gap junctional conductances from macroscopic double whole-cell recordings. These results also constitute empirically determined estimates of the open probability that are not model-dependent.

Key words: Gap junction — Noise analysis — Non-stationary — Uncoupling — Macroscopic — Conductance — Gating

Introduction

Spanning as they do two bilayers, high-resolution recordings of gap junction channels have always posed a problem, arising from the fact that the recording of gap junction channel currents requires the use of the double whole-cell patch-clamp (DWCP) technique, where two closely apposed cells are simultaneously clamped in the whole-cell or perforated-cell mode (Neyton & Trautmann, 1985; Takens-Kwak & Jongsma, 1992). Under appropriate ionic and pharmacological conditions, a voltage step applied to one cell of a pair elicits currents from the two apposed cells that are of equal but opposite sign, as a result of current flow through gap junction channels. Only rarely are single channels recorded; most often, multichannel or macroscopic records are obtained. This is opposed to the situation for almost all other ion channels that span only one bilayer (Hille, 1992), where, in attached or detached patches, single channels can be routinely recorded. This inability to record gap junction channels in the detached mode reduces the probability of recording true single-channel activity. In fact, DWCP most often results in the simultaneous activity of a number of channels; typically only one in 10–20 DWCP records is a single-channel patch in transfected cells, and in some systems, such as ventricular cardiomyocytes, single-channel recordings are virtually impossible both due to the low whole-cell resistance as well as the expression of thousands of gap junction channels.

There are at least 20 different isoforms of the basic subunit of the gap junction channel, the connexin (Cx; Beyer, 1993; Willecke et al., 2002). It is possible to transfect connexins into cells and subsequently select clones for functional studies. This has been accomplished for homotypic gap junction channels and some hetero-oligomeric forms as well (Veenstra et al., 1994; White and Bruzzone, 1996; He et al., 1999; Valiunas, Weingart and Brink, 2000). One of the most successful tools for studying the conductive or permeation pathway of the potassium channel (Dun, Jiang & Tseng, 1999; Lu et al., 2001), for example, has been site-directed mutation where single-channel recording is routine. Unfortunately, monitoring single channels to assess the effects of mutations is problematic in the case of gap junction channels, as most recordings reflect the activity of many channels. Such macroscopic recordings, while useful for analysis of channel kinetics, do not yield information about single-channel conductances. However, there does exist a technique for extracting single-channel conductance from macroscopic records, namely fluctuation analysis (Sigworth, 1980). In this paper, we show that this method can be

Correspondence to: S.V. Ramanan; email: ramanan@au-kbc.org

applied, with some minor modifications, to gap junction records as well.

An additional advantage of this method is that it also allows an estimate of the open-channel probability of the channel at low transjunctional voltages, which is not model- or assumption-dependent. Gap junction channels are composed of a series combination of two gating hemichannels, and traditional analysis of macroscopic records of junctional currents have used the ratio of steady-state to instantaneous current as a relative measure of the open probability. Boltzmann fits of the form $1/(1+\exp(z(V\text{-}V_0)))$ are then applied separately to each side (i.e., $V_j<0$ and $V_j>0$) of the G_j/V_j curve, assuming that the gating of the two hemichannels does not overlap, i.e., that the gap junction channels are fully open at $V_j = 0$. Here, G_j is the junctional conductance and V_j is the applied transjunctional voltage. This is equivalent to assuming that the absolute value of $|zV_0| >> 0$, where z is the hemichannel gating charge and V_0 is the transjunctional voltage at which the channels have a probability of opening of half. However, it is entirely possible that some gap junction channels, especially mutated constructs, will have gating characteristics such that the open probability of the whole channel is less than 1 at zero transjunctional voltage, especially if $|zV_0| \sim 0$. Fluctuation analysis can help to discriminate between these alternatives from macroscopic records alone, as it provides a direct measure of the open probability of the channel.

Chen-Izu, Moreno and Spangler (2001) have systematically fit data from GJ records by using the product of two Boltzmanns, one for each hemichannel. This analysis overcomes the limitations of fitting with a single Boltzmann mentioned in the above paragraph. However, there is an implicit assumption that the two hemichannels gate independently. An estimate of the probability from fluctuation analysis imposes no restrictions on the mechanism of gating of an individual channel. The method works as long as channels in a given macroscopic record can be assumed to gate independently.

We have applied the fluctuation analysis method to human Cx37 and rat Cx43 expressed in RIN cells. The approach accurately predicts single-channel conductances from homotypic channels with unitary conductances ranging from tens of pS (45 pS for Cx43; Moreno et al., 1994; Valiunas, Bukauskas & Weingart, 1997; Burt & Spray, 1988; Valiunas et al., 2000) to hundreds of pS (Cx37; ~300 pS; Veenstra et al., 1994; Ramanan et al., 1999), and their expression ranges from tens (Cx37) to hundreds of channels (Cx43). The method produces results comparable to those seen in single-channel records. It should be noted that the conductances given here are only for voltage-dependent transitions, as voltage-independent transitions would produce a fluctuation component indistinguishable from background noise. The open probabilities of the channels at $V_j = 0$ are all in the range of unity, i.e., $|zV_0| >> 0$ for both channel types. This is also consistent with results from single-channel recordings. A preliminary report on these results has been presented (Brink, Valiunas & Ramanan, 1999).

Materials and Methods

Experimental

The methods for DWCP have been described elsewhere (Valiunas, Beyer & Brink, 2002). All recordings were done in 110 mM CsCl saline. We used double whole-cell patch clamp to monitor junctional conductance (Neyton & Trautmann, 1985). For all double whole-cell patch-experiments, the extracellular perfusate was a Na-saline containing 110 mM NaCl, 1 mM $MgCl_2$, 2 mM $CaCl_2$, 10 mM HEPES at pH = 7.4. The pipette solution contained 110 mM CsCl or KCl, 1 mM $MgCl_2$, 0.1 mM $CaCl_2$, 1 mM EGTA, 1 mM ATP, and 10 mM HEPES at pH 7.2. We used standard patch methods to apply protocols as shown in Fig. 1. The recordings were made on RIN cells transfected with Cx37 and Cx43.

Data Collection

Voltage steps were administered and current traces were collected with a DT21EZ A/D board (Data Translation, Marlboro, MA using a customized program. The data was sampled at 100 microseconds after (analog) low-pass filtering at 100 Hz.

In a typical step regime, both patched cells were held at zero transjunctional potential. A 5 mV transjunctional pre-step was given for 100 ms, after which V_j was restored to zero for another 100 ms. The potential was then set to a transjunctional voltage high enough for the channel to close completely by the end of the step (400 ms steps). The voltage was then clamped low again (but not zero) to open the channel (also 400 ms). The voltage was then restored to zero for a long enough time (2–5 s for Cx37 and 5 s for Cx43) so that the channel could be restored to equilibrium before repetition of the stepping regime.

Analysis

If the mean current were somehow known precisely, finding the variance from a current trace would be trivial. In Sigworth (1980), the mean was found by averaging over successive 4, 10 or 20 current records X_i in a moving window. This helped eliminate the problem of long-term drift. Noceti et al., (1996) used the variable $Y_i = X_{i+1} - X_i$ instead, effectively limiting the computation of the local mean to 2 successive records.

Most gap junction records suffer from irreversible rundown upon successive steps. In RIN cells, anywhere between 10 and 40 traces can be obtained before the cells uncouple completely. The mechanism that causes this rundown is not known. Regardless of the cause, both the schemes mentioned above behave somewhat erratically in the presence of rundown. If the number of junction channels decreased linearly with time, we could overcome this by a central differencing scheme with variable $Y_i = X_{i+1} + X_{i-1} - 2X_i$. Here we are effectively averaging over three successive traces.

We have modified this last scheme to account for non-linear rundown. In this, we are assisted by the fact that the current for the small 5 mV prestep is a rough measure of the total conductance for the following step, and can be used as a normalizing factor. Writing P_1, P_2, ..., P_k, for the currents for the k successive pre-steps, the variables Y_i are now defined to be

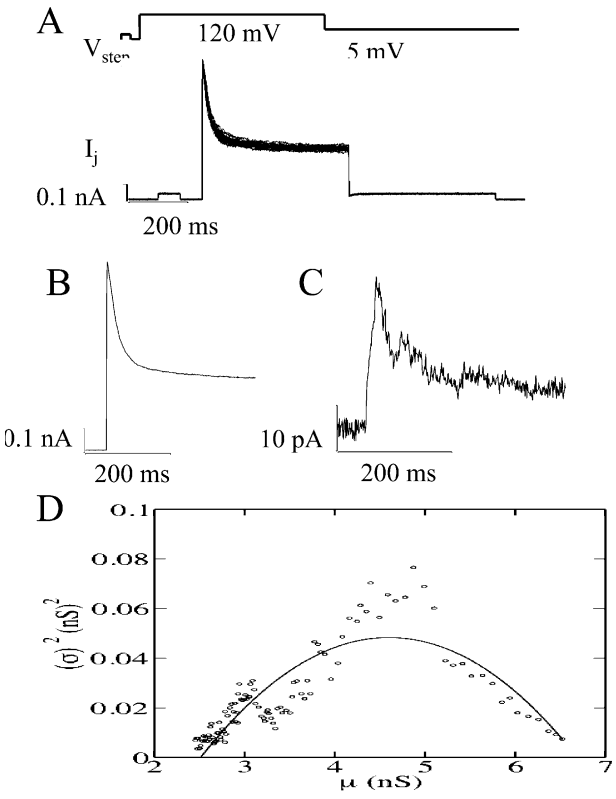

Fig. 1. Panel *A* shows junctional currents (I_j) from the recipient cell of a Cx43-transfected pair upon imposition of a voltage protocol (*V*step) to the other cell, the stepped cell. From a holding transjunctional voltage V_j of 0 mV, a prestep of 5 mV was applied for 40 ms before V_j was returned to 0 mV for 200 ms. The current upon the prestep provides a convenient indicator of the number of active channels during the step, which is useful for the analysis. A voltage step of 120 mV was then applied for 500 ms, and the current gradually reduced to a residual value as the channel gates closed. A post-step of 5 mV was applied for another 500 ms during which the channel opened again, before V_j was returned to zero. The currents during both the step and the post-step regimes can be used for the fluctuation analysis. The step regime was applied 20 times. Panels *B* and *C* show the mean (panel *B*) and the associated fluctuation noise (the square root of the variance) during the entire protocol. The variance (panel *C*) was extracted from the data by the modified centered difference discussed in the text. The fluctuations increase as the channels actively start gating to the closed state, only to diminish again as gating activity decreases when the channel closes completely to the residual state by the end of the main step to 120 mV. Panel *D* shows the variance from the data of *A* plotted against the mean (for the 120 mV pulse), both in conductance units (nS). The heavy line is the best fit from Eq. 1 in the text. The fit produces a value of 46 pS for the single-channel transition conductance, which is comparable to that observed directly in single-channel recordings.

$$Y_i = X_{i+1} + X_{i-1} - ((P_{i+1} + P_{i-1})/P_i)X_i, i = 2, 3, ...k-1$$

Note that

$$< Y_i > = < X_{i+1} > + < X_{i-1} > - ((P_{i+1}+P_{i-1})/P_i) < X_i >$$
$$= pI(N_{i+1}+N_{i-1}-((P_{i+1}+P_{i-1})/P_i)N_i),$$

since $< X_i > = N_i\, I\, p$, where N_i is the number of channels at the ith step, I is the single-channel current, and p is the open probability.

Since $P_{i+1}/P_i = N_{i+1}/N_i$ if the current at the prestep is to reflect the number of active channels at the step, we get $< Y_i > = 0$ as desired. Further,

$$< Y_i^2 > = < P_{i+1}^2 > + < P_{i-1}^2 > + ((P_{i+1}+P_{i-1})/P_i)^2 < X_i^2 >$$

assuming, as usual, that the X_i's are uncorrelated. Using $< X_i^2 > = N_i pqI^2$ with $q = 1-p$, we get

$$< Y_i^2 > /(pqI^2) = N_{i+1} + N_{i-1} + ((P_{i+1} + P_{i-1})/P_i)^2 N_i$$
$$= (N_{i+1} + N_{i-1})(1 + (P_{i+1} + P_{i-1})/P_i)).$$

Define

$$Z_i = 0.5 < Y_i^2 > /(1 + (P_{i+1}+P_{i-1})/P_i)$$

where the right-hand side contains only experimentally measured quantities. It follows that

$$\Sigma_i Z_i = 0.5(N_1+N_2+2N_3+...+2N_{k-2}+N_{k-1}+N_k)pqI^2.$$

Defining the variance σ^2 by

$$\sigma^2 = (1/k)(N_1+N_2+...+N_k)pqI^2 = NpqI^2$$

we find approximately that

$$\sigma^2 \approx (1/(k-2))\Sigma(Z_i)$$

The mean μ is calculated directly from the original X's by the equation

$$\mu = (1/k)(X_1 + X_2 + ... + X_k)$$
$$\mu = (1/k)(N_1+N_2+...+N_k)pI = NpI$$

where N is the mean number of channels over the recording period. Then it is still true that

$$\sigma^2 = (1/k)(N_1+N_2+...+N_k)pqI^2 = \mu I - \mu^2/N \quad (1)$$

In practice, we also calculate the variance at $V = 0$ and subtract this background variance from the variance of the Y_i's.

Gap junction channels invariably possess a long-lived substate or residual state (Veenstra et al., 1994; Bukauskas et al., 1995). The major gating transition of the channel is from the open state to this residual state, and further gating to true closure is often a sign of channel rundown (Bukauskas et al., 1995). This affects Eq. 1 only in that I is replaced by $I-I_0$, where I_0 is the current in the residual state. In terms of conductance, the conductance G of the channel is given by

$$G = G_{trans} + G_{res}$$

where G_{trans} is the conductance associated with the transition from open to residual state, and G_{res} is the conductance of the residual state. The currents are then $I = NVG$, $I_0 = NVG_{res}$, where V is the applied transjunctional potential.

The maximum open probability p_{max} can be extrapolated from the maximum observed mean current I_{max} as

$$p_{max} = (I_{max} - I_0)/(NI)$$

Assumptions Underlying The Above Analysis

There are several assumptions that underlie the above analysis. Three key assumptions are applicable to all methods that use non-stationary methods to extract single-channel information. The first is the assumption that all the channels being recorded from are homogeneous. Specifically, channels should be identical in both conductance and gating behavior. Heterogeneity in either of these parameters usually results in a distortion of the parabolic profile of

the mean-variance plot. Practically, this means that, for connexin channels, the analysis is best applied to channels that are formed of only one connexin. For hetero-oligomeric channels, the analysis requires that the stoichiometry should be tightly regulated, although variations in the geometric disposition of the different subunits may still confound its application. It should be noted that, even for identical channels, heterogeneity in function may yet arise from differential phosphorylation levels due to spatial heterogeneities in associated kinases.

A second common assumption is that the channels gate independently of one another. If channels gate cooperatively, then the single-channel conductances that are predicted by the analysis will be greater than the true single-channel conductance, as determined by the number of channels in the functional cooperative unit. There is some evidence (Valiunas & Weingart, 2001) that gap junction channels may gate cooperatively in certain circumstances; however, it would seem that gating independence is the norm in the majority of recordings from gap junction channels.

A third assumption is that the current fluctuations arise only from the channels under study. As we analyze only junctional currents from the non-stepped cell in the DWCP configuration, we can ignore transient evoked currents from non-junctional channels in the stepped cell. We ignore noise from thermal sources, as it is about two orders of magnitude lower than gating noise (Sigworth, 1985). However, thermal noise increases quadratically with current and is maximal when the channels are completely open. This fact can be used to distinguish it from gating fluctuations that have a parabolic profile with increasing current.

There are also caveats regarding the particular analysis presented here. For example, the analysis assumes that run-down is all-or-none at the single-channel level, i.e., a channel is either active during a record or it is completely silent. Channels that have long silent "modes" of several minutes (Brink, Ramanan & Christ, 1996) will lead to erroneous analysis. Another potential problem arises due to the contribution from substates. The analysis assumes that gap junction channels, similar to other channels, have only two states, an open and a closed state. While the analysis can accommodate a non-zero current flowing through the "closed" substate, it is assumed that there is no further gating activity to the true zero-current state. Several connexin channels are known to violate this assumption (loop gating; Trexler et al., 1996; Harris, 2001). In fact, most connexin channels have a multiplicity of conducting states.

Many of these shortcomings of the analysis may account for some of the variances in the results, which are noted in the discussion below.

Practical Shortcomings

A minimum of ten consecutive repetitive steps seems to be necessary for applying the analysis to data from gap junction channels. We have observed that some records show unexplainable changes in the middle of a recording for two or so steps, following which the channels revert to more typical behavior. If the number of steps exceeds 20 or so, the results obtained by omitting these aberrant steps from the analysis are comparable to results from more "normal" records.

Good seals are also a requirement for analysis of macroscopic records from gap junction channels. Junctional conductances are often in the range of 5–20 nS, and the seals should be better than 500 Megaohms for each of the two electrodes in the DWCP configuration for reliable estimates of conductances as well as gating behavior. These seal resistances are best estimated by the amplitude and time constants of short steps applied to each of the cells in turn.

Optimizing the parameters for fitting the mean-variance plots was done by the use of the FDJAC algorithm from LINPACK as integrated into the Xmgrace package. This routine is quite robust, although it functions better if some thinning is used against data from the steady state at the end of the pulse, which tends sometimes to be large compared to the data from the transient regime.

Results

Figure 1*A* shows data from a RIN cell pair transfected with rat Cx43. In one cell of a coupled pair, a step voltage of 120 mV was applied and immediately followed by a post-pulse of 5 mV. A small pre-pulse of 5 mV preceded the (120 and 5 mV) step protocol. There was not much rundown in this recording. Nevertheless, the junctional current from the 5 mV pre-pulses was used to correct for this rundown for the purposes of fluctuation analysis.

Figure 1*B* shows the mean and Fig. 1*C* shows the square root of the variance as a function of time during the 120 mV pulse. Note that the variance increases to a peak and then decreases again during the pulse. This noise arises from the stochastic nature of channel gating, and is maximal when the open probability is half. The variance thus has a maximum when the channel probability crosses half during its decrease from a large value at the beginning of the 120 mV step (from 0 mV) to close to zero at the end of the step.

Figure 1*D* plots the variance against the mean (both in conductance units) for the 120 mV step. The continuous line is the fit from Eq. 1 above. The optimized parameters for the fit are $G_{trans} = 46$ pS, $G_{res} = 28$ pS and $N = 92$. The total conductance G has a value of 74 pS (46 + 28 pS), which is close to the single-channel conductance of 74 pS (45 + 29 pS) in 110 mM CsCl (Valiunas et al., 2000). Other DWCP studies give similar results when corrected for salt concentration (Burt & Spray, 1988; Moreno et al., 1994; Valiunas et al., 1997). From the peak conductance observed in the data, we can calculate p_{max} to be 0.85. This peak in probability (and current) occurs at the start of the pulse and corresponds to the equilibrium open probability at the transjunctional voltage preceding the pulse, which was zero.

Figure 2 shows similar data from another cell pair for Cx43 channels. However, the rundown is quite prominent in this recording, with the final peak currents (after 14 steps) being only about 40% of the peak current on the first step. In this recording, a step voltage of 90 mV was applied, immediately followed by a post-pulse of 20 mV, with a 5 mV pre-pulse. Again, the junctional current from the pre-pulses was used to correct for this rundown for the purposes of fluctuation analysis using a central difference scheme.

Figure 2*B* shows the mean and Fig. 2*C* shows the square root of the variance as a function of time. In this figure, it can be seen that the variance has a peak both when the channel probability falls from a large value (at the beginning of the 90 mV step) to close to

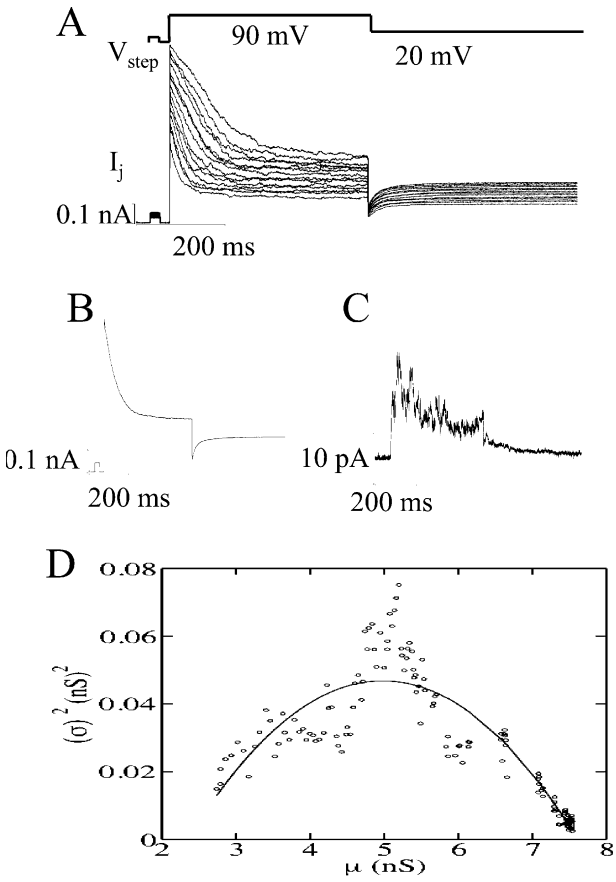

Fig. 2. A recording from Cx43 channels that is similar to that in Fig. 1, but with rundown. Panel *A* shows junctional currents. The protocol is similar to that in Fig. 1, except that a voltage step of 90 mV is followed by a post-step of 20 mV before V_j is returned to zero. The step regime was applied 14 times during which the junctional current reduced by ~70% in magnitude. Panels *B* and *C* show, respectively, the mean and the associated fluctuation noise. The fluctuations increase and decrease again, both, during the step to 90 mV as well as during the post-step of 20 mV. Panel *D* plots the variance against the mean for the 20 mV pulse; the heavy line is the best fit from Eq. 1 in the text. Notwithstanding the rundown, the fit predicts that the transition conductance is 36 pS, only about 20% off the directly observed value.

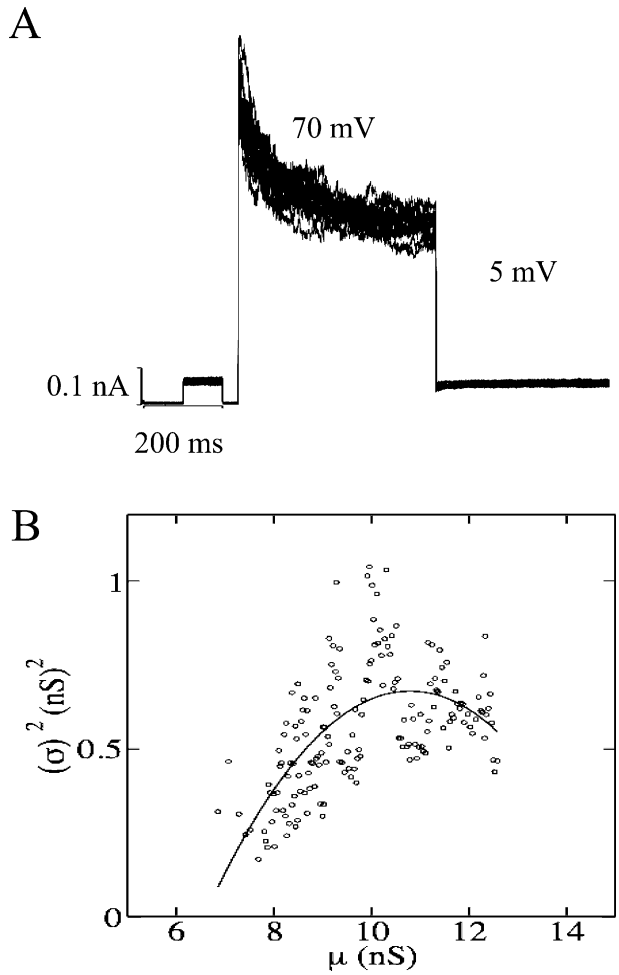

Fig. 3. Panel *A* shows the raw macroscopic data and Panel *B* shows the variance-mean plot from a record of junctional current from Cx37 channels (70 mV and 5 mV steps). The predicted value for the Cx37 transition conductance from the optimized fit (dark line) is 320 pS; this matches single-channel values of 300 pS in the literature.

zero (at the end of the step) as well as when the probability increases to a large value during the 20 mV post-pulse. Figure 2*D* plots the variance against the mean (both in conductance units) for the 20 mV step. The continuous line is the fit from Eq. 1 above. The optimized parameters for the fit are G_{trans} = 36 pS, G_{res} = 16 pS, N = 148 and p_{max} = 0.98. Even with extreme rundown, the transition conductance is predicted to within 20% of the directly observed value by fluctuation analysis.

Panel *A* of Fig. 3 shows a recording from a cell pair with Cx37 channels. Panel *B* shows the variance-mean plot for this recording with 16 traces. The analysis showed that G_{trans} was 320 pS, G_{res} = 240 pS and N = 26, while p_{max} was 0.71. Again, the prediction transition conductance is close to the directly observed value of 300 pS from single-channel studies. It may be noted that the number of Cx37 channels (average N = 18) in these transfected cells is far less than the corresponding number of Cx43 channels (average N = 123). We note that the number of channels, N, in patches where there is rundown, is defined to be the mean number of channels during the recording time (please *see* text preceding Equation 1).

Table 1 summarizes the results. The mean transition conductances for Cx43 and Cx37 fall within the range observed directly from DWCP of pairs with low numbers of junctional channels. However, the value for the residual conductance for Cx37 (in particular) seems high, and residual conductances for both connexins have high standard deviations (SD) associated with them. A possible explanation is that many Cx37 channels reside for long times in the residual state (Ramanan et al., 1999) and skew the

Table 1. Conductances and open probabilities of Cx43 and Cx37 channels from fluctuation analysis

Connexin	*M*	$G_{junctional}$	G_{trans} *(pS)*	G_{res} *(pS)*	p_{max}
Cx43	12	8.45	43 ± 17	18 ± 12	0.95 ± 0.06
Cx37	9	7.43	278 ± 101	178 ± 90	0.81 ± 0.15

M is the number of observations; $G_{\text{junctional}}$ is the junctional conductance of the patch; G_{trans} is the conductance associated with the transition from open to residual state referred to as the transition conductance; G_{res} is the conductance of the residual state and $p_{\max}$ is the maximal open probability of the channel during the voltage step. For comparison, the values of the transition conductance (G_{trans}) from direct DWCP recordings are: Cx43, 45pS; Cx37, 300 pS.

predictions from the analysis to large values (*see* Discussion below).

The maximal open probability of both channel types is large at low transjunctional voltages, certainly greater than 0.7. This confirms results reported in the DWCP literature for Cx43 and Cx37 (Veenstra et al., 1994; Valiunas et al., 1997; Valiunas et al., 2002).

Discussion

The method presented here does accurately predict transition conductances (G_{trans}) in the range observed in single-channel measurements by the DWCP method. It would seem that it can be therefore applied to macroscopic recordings from oocytes as well as transfected cells. However, there are some shortcomings in this approach, which are discussed below (please also *see* the Methods section for additional discussion).

It is useful to define a "rundown" parameter as the ratio of the minimum to the maximum current observed in the 5 mV prestep regime. This parameter varied from 0.52 to 0.95 for Cx43 channels, and had a mean value of 0.77. By contrast, for Cx37 channels, the rundown varied between 0.17 and 0.71 and had a mean value of 0.47. In both cases, the method presented here predicts transition conductances that can be seen from Table 1 to be within ~7% of the conductance observed by the direct DWCP method. This lends support to our premise that the method does work in compensating for the extreme rundown often seen in gap junction records.

Poor seal resistances and high series resistances pose a problem in estimating conductance even in single-channel recordings, and this problem is exacerbated in macroscopic recordings. For example, typical junctional conductances are of the order of about 5–20 nS. If seal or series resistances are comparable to this value, the junctional transition conductances (G_{trans}) would be underestimated because of two reasons: (1) part of the junctional current would leak out of the seal resistance and (2) the applied voltage would be different from that across the junction (Wilders & Jongsma, 1992; Veenstra, 2001; Musa & Veenstra, 2003). In DWCP recordings, the transition conductances are 45 and 300 pS for Cx43 and Cx37, respectively, in 110 mM CsCl saline. Table 1 records the same values as 43 and 278 pS, a reduction of approximately 7%. This is compatible with the expected drop of about 5% from the series resistance of the two patch pipettes, which is about 3 MΩ ohms for each pipette, and a junctional conductance of 10 nS. We note that it is possible to use the analysis in Veenstra (2001) to estimate the true junctional conductance, given knowledge of the seal and series resistances. In this work, we have chosen datasets where artifacts due to seal and series resistances are minimal.

The series resistance problem would affect the residual conductances less, as their conductances are 3- to 4-fold lower than the transition conductances. This may partly account for the high residual conductances observed for Cx37, where the transition conductance is very high (~300 pS). However, junctional channels that close to the residual state also remain for long periods in this state, from which they either reopen or even disappear altogether (Brink et al., 1996; Ramanan et al., 1999). Thus, repeated pulses to high potentials not only cause or trigger uncoupling but also result in an overestimate of the conductances of the substates. It seems best, therefore, to obtain only the transition conductance (G_{trans}) from a fluctuation analysis.

The maximum gap junction channel open probability for Cx43 is approximately 0.95 using fluctuation analysis, which is similar to the values derived from macroscopic data using Boltzmann fits (Chen-Izu et al., 2001). Using microscopic data (a few channels), the open probability for human Cx43 in vascular smooth muscle cell pairs has been experimentally determined under steady-state conditions by measurement of mean open and closed times, yielding a value of 0.64 (Brink et al., 1996, Fig. 6 therein).

The differences between these data are most probably due to a loss of a specific population or number of high-open-probability channels in the multichannel data over the time to reach steady state. The latter was the argument invoked by Brink et al. (1996) to explain the reduction and subsequent recovery of 25 or more observed channels at the onset of a transjunctional potential, which in steady state reduced to only 4 or 5 observable channels.

The maximum open probability for Cx37 was 0.81 using fluctuation analysis. This value is midway between the value given by Chen-Izu et al., (2001) of 0.9 using a Boltzmann fit, and that of Ramanan et al., (1999, Figs. 2 and 4 therein), which was 0.71 for macroscopic data and 0.5 based on microscopic data. The same arguments made for the discrepancies in the Cx43 data can be applied to the Cx37 data. In general, all the open-probability data are consistent with a channel type for Cx43 and Cx37 that remains open more than closed under physiological conditions (i.e., $V_j = 0$ mV).

As the method presented here derives parameter estimates in the presence of rundown, we examined the results for correlations between rundown (as defined in the beginning of this section) and estimates of the transition conductance, the residual conductance and the open probability. As expected, the confidence levels for all correlations were low, except for that between the transition conductance for Cx43 and rundown (correlation $r = -0.66$; confidence level = 0.027). Apparently, the method does not completely correct for rundown in the case of smaller Cx43 conductances, where fluctuations associated with channel transitions are lower (please *see* Eq. 1) than for the larger conductances associated with Cx37. In any case, the conductance of Cx43 channels as estimated by this method could be used as a lower bound for the unitary transitions.

Some mutant connexin channels have a flickery behavior, i.e., devoid of the long open and closed states that permit direct observation of unitary conductances in DWCP recordings. In macroscopic recordings of such channels, the low-pass filter bandwidth is generally kept to 1 kHz (or lower) to reduce noise contributions from pipette and background sources. In a scenario where mutant channels have fast microsecond flickering, fluctuation analysis would predict a conductance that is less than the real value. Increasing the filter bandwidth to observe fast transitions would introduce background noise, which would drown out fluctuations due to channel transitions. Additionally, if flickering varied with voltage, there would be a bias in the data towards those voltages where the transitions were the slowest. If, for example, flickering is fastest when the channel is "half-open" (where unitary transitions are the most frequent), then the fluctuation noise from channel transitions would be compromised by the "flickering noise" from low filter bandwidth. Practically, it would seem that gap junction channels with transition times of the order of 1–10 ms or less would not be good candidates for fluctuation analysis from DWCP records.

In spite of these shortcomings, fluctuation analysis is applicable to gap junction channels and produces estimates of single-channel transition conductances to within 7% of directly measured values. This method offers a rapid approach to screening for changes in the channel permeation pathway (transition conductances) as well as maximal open probabilities from macroscopic recordings. The method can be used to quickly check for channel susceptibility to phosphorylation or to select promising mutants for detailed single-channel study.

We thank the reviewers for their comments. This work was, in part, funded by Wellcome Trust grant 070069 (SVR) and NIH grant 55263 (PRB).

References

Beyer E.C. Gap junctions. 1993. Intl. Rev. Cyto. 137C:1–37

Brink, P.R., Ramanan, S.V., Christ, G.J. 1996. Human connexin43 gap junction channel gating: evidence for mode shifts and/or heterogeneity. *Amer. J. Physiol.* **271:**C321–C331

Brink, P.R., Valiunas, V., Ramanan, S.V. 1999. High open probability demonstrated through non-stationary noise analysis in three gap junctions. International gap junction conference, Bern, Switzerland,

Bukauskas, F., Bukauskiene, A.A., Verselis, V.K., Bennett, M.V.L. 2002. Coupling asymmetry of heterotypic connexin45/connexin43-EGFP gap junction: Properties of fast and slow gating mechanisms. *Proc. Nat. Acad. Sci. USA* **99:**7113–7118

Bukauskas, F., Elfgang, C., Willecke, K., Weingart, R. 1995. Biophysical properties of gap junction channels formed by mouse connexin40 in induced pairs of transfected HeLa cells. *Biophys. J.* **68:**2289–2298

Burt, J.M., Spray, D.C. 1988. Inotropic agents modulate gap junctional conductance between cardiac myocytes. *Amer. J. Physiol.* **254:**H1206–H1210

Chen-Izu, Y., Moreno, A.P., Spangler, S.R.A. 2001. Opposing gates model for voltage gating of gap junction channels. *Amer. J. Physiol.* **281:**C1604–C1613

Dun, W., Jiang, M., Tseng, G.N. 1999. Allosteric effects of mutations in the extracellular S5-P loop on the gating and permeation properties of the hERG potassium channel. *Pfluegers Arch.* **439:**141–149

Harris, A.L. 2001. Emerging issues of connexin channels: biophysics fills the gap. *Quart. Rev. Biophys.* **34:**325–472

He, D.S., Jiang, J.X., Taffet, S.M., Burt, J.M. 1999. Formation of heteromeric gap junction channels by connexins 40 and 43 in vascular smooth muscle cells. *Proc. Natl. Acad. Sci.* **96:**6495–6500

Hille, B. 1992. Ionic channels of excitable membranes. 2nd ed. Sinauer Associates, Inc. Sunderland, Ma

Lu, T., Ting, A.Y.M., Mainland, J., Jan, L.Y., Schultz, P.O., Yang, Y. 2001. Probing ion permeation and gating in a K^+ channel with backbone mutations in the selectivity filter. *Nat. Neurosci.* **4:**239–246

Moreno, A.P., Rook, M.R., Fishman, G.I., Spray, D.C. 1994. Gap junction channels; distinct voltage sensitive and insensitive conductance states. *Biophys J.* **67:**113–119

Musa, H., Veenstra, R.D. 2003. Voltage-dependent blockade of connexin40 gap junctions by spermine. *Biophys. J.* **84:**205–219

Neyton, J., Trautmann, A. 1985. Single channel currents of an intercellular junction. *Nature.* **317:**331–335

Noceti, F., Baldelli, P., Wei, X., Qin, N., Toro, L., Birnbaumer, L., Stefani, E. 1996. Effective gating charges per channel in voltage-dependent $^{K+}$ and Ca^{2+} channels. *J. Gen. Physiol.* **108:**143–155

Ramanan, S.V., Brink, P.R., Varadaraj, K., Peterson, E., Schirrmacher, K., Banach, K. 1999. A three-state model for connexin37 gating kinetics. *Biophys. J.* **76:**2520–2529

Sigworth, F.J. 1985. Open channel noise. I. Noise in acetylcholine receptor currents suggests conformational fluctuations. *Biophys J.* **47:**709–720

Sigworth, F.J. 1980. The variance of sodium currents at the node of Ranvier. *J. Physiol.* **307:**97–129

Takens-Kwak, B.R., Jongsma, H.J. 1992. Cardiac gap junctions: three distinct single channel conductances and their modulation by phosphorylating treatments. *Pfluegers Arch.* **422:**198–200

Trexler, E.B., Bennett, M.V.L., Bargiello, T.A., Verselis, V.K. 1996. Voltage gating and permeation in a gap junction hemichannel. *Proc. Nat. Acad. Sci. USA* **93:**5836–5841

Valiunas, V., Beyer, E.C., Brink, P.R. 2002. Cardiac gap junction channels show quantitative differences in selectivity. *Circ. Res.* **91:**104–111

Valiunas, V., Bukauskas, F., Weingart, R. 1997. Conductances and selective permeability of connexin43 gap junction channels examined in Neonatal rat heart cells. *Circ. Res.* **80:**708–719

Valiunas, V., Weingart, R., Brink, P.R. 2000. Formation of heterotypic gap junction channels by connexins Cx40 and Cx43. *Circ. Res.* **86:**e42–e49

Valiunas, V., Weingart, R. 2001. Co-operativity between mouse connexin30 gap junction channels. *Pfluegers Arch.* **441:**756–760

Veenstra, R.D., Wang, Z., Beyer, E.G., Ramanan, S.V., Brink, P.R. 1994. Connexin37 forms high conductance gap junction channels with subconductance state activity and selective dye and ionic permeabilities. *Biophys. J.* **66:**1915–1928

Veenstra, R.D. 2001. Voltage clamp limitations of dual whole-cell gap junction current and voltage recordings. I. Conductance measurements. *Biophys. J.* **80:**2231–2247

White, T., Bruzzone, R. 1996. Multiple connexin proteins in single intercellular channels: connexin compatability and functional consequences J. *BioEner. Biomembranes.* **28:**339–350

Wilders, R., Jongsma, H. 1992. Limitation of the dual voltage clamp method in assaying conductance and kinetics of gap junction channels. *Biophys. J.* **63:**942–953

Willecke, K., Eiberger, J., Degan, J., Eckardt, D., Romualdi, A., Guldenagel, M., Deutsch, U., Sohl, G. 2002. Structural and functional diversity of connexin genes in the mouse and human genome. *Biol. Chem.* **383:**725–737